Feasibility of 100% renewable energy-based electricity production for cities with storage and flexibility

Narayanan Arun, Mets Kevin, Strobbe Matthias, Develder Chris

DOI: 10.1016/j.renene.2018.11.049

Feasibility of 100% Renewable Energy-based Electricity Production for Cities with Storage and Flexibility

Arun Narayanan[a,1,*], Kevin Mets[b,2], Matthias Strobbe[b], Chris Develder[b]

[a]*School of Energy Systems, Lappeenranta University of Technology, Lappenranta, Finland 53850*
[b]*IDLab, Dept. of Information Technology, Ghent University—imec, Ghent, Belgium 9052*

Abstract

Renewable energy is expected to constitute a significant proportion of electricity production. Further, the global population is increasingly concentrated in cities. We investigate whether it is possible to cost-effectively employ 100% renewable energy sources (RES)—including battery energy storage systems (BESS)—for producing electricity to meet cities' loads. We further analyze the potential to use only RES to meet *partial* loads, e.g., by meeting load demands only for certain fractions of the time. We present a novel flexible-load methodology and investigate the cost reduction achieved by shifting fractions of load across time. We use it to evaluate the impacts of exploiting *flexibility* on making a 100% RES scenario cost effective. For instance, in a case study for Kortrijk, a typical Belgian city with around 75,000 inhabitants, we find that from a purely economic viewpoint, RES–BESS systems are not cost effective even with flexible loads: RES–BESS costs must decrease to around 40% and 7% (around 0.044 €/kWh and 0.038 €/kWh), respectively, of the reference levelized costs of electricity to cost-effectively supply the city's load demand. These results suggest that electricity alone may not lead to high penetration of RES, and integration between electricity, heat, transport and other sectors is crucial.

Keywords: Renewable energy sources, Linear programming, Electricity production, Partial Loads, Flexible loads

Nomenclature

*Principal corresponding author
Email address: arun.narayanan@lut.fi (Arun Narayanan)

[1]Narayanan conducted a part of this research at the Dept. of Information Technology—IBCN, Ghent University, Ghent, Belgium 9050.

[2]Dr. Mets is currently working at the University of Antwerp—IMEC IDLab Research Group, Middelheimlaan 1, Antwerp, Belgium 2020.

α	Percentage of flexible load shifted across $r-1$ time steps, %
$b_t = [b_1, ..., b_T]$	Binary decision variables, $b_t \in \mathbb{Z}_2$
B_{max}	Maximum battery energy storage system (BESS) capacity, Wh
$B(t) = [B(t_1), ..., B(t_T)]$	BESS capacity, Wh
$B_\Delta(t)$	Difference in BESS capacity, $B_t - B_{t-1}$, Wh
C_b	Levelized cost of energy (LCOE) for BESS, monetary unit/Wh
C_{pv}	LCOE for photovoltaic (PV) panels, monetary unit/Wh
C_w	LCOE for wind turbines, monetary unit/Wh
C_g	LCOE for non-renewable energy sources, monetary unit/Wh
δ	Proportion of the load demand that is flexible
$E_l(t) = [E_l(t_1), ..., E_l(t_T)]$	Load energy, Wh
$E_{fl}(t) = [E_{fl}(t_1), ..., E_{fl}(t_T)]$	Flexible load energy, Wh
$E_{infl}(t) = [E_{infl}(t_1), ..., E_{infl}(t_T)]$	Inflexible load energy, Wh
E_g	Energy produced by non-renewable energy sources, Wh
E_{pv}	Energy produced by PV installations, Wh
E_w	Energy produced by wind turbine installations, Wh
$f_{pv}(I(t))$	Function that converts $I(t)$ to solar energy
$f_w(W_s(t))$	Function that converts $W_s(t)$ to wind energy
$I(t) = [I(t_1), ..., I(t_T)]$	Solar irradiation, Wh/m^2
k_{ch}	BESS charge rate
k_{dch}	BESS discharge rate
r	Number of time steps across which flexible load can be shifted
T	Total time period
$t_i = [t_1, ..., t_T]$	Time steps
T_k	Total time steps with electric power
$W_s(t) = [W_s(t_1), ..., W_s(t_T)]$	Wind speed, m/s

1. Introduction

Climate change concerns and increasing environmental awareness have encouraged governments, industries, and researchers to make considerable efforts to reduce the current dependence on traditional non-renewable energy sources (NRES), such as fossil fuels, by focusing on alternative renewable energy sources (RES) of electricity production, such as solar and wind energy. The European Union (EU), for example, has set ambitious targets for 2030—to reduce greenhouse gas emissions by 40% compared to 1990, to ensure a share of at least 27% of renewable energy, and to achieve at least 27% energy savings compared to business-as-usual scenarios [1].

Global energy demand is expected to increase by nearly 30% from 2016–2040, of which electric load demand will account for almost 40% of the additional consumption until 2040. At the same time, RES will comprise nearly 60% of all new electricity production capacity up to 2040 [2]. RES are also becoming cost-competitive with NRES. From 2009–2014, the levelized cost of electricity (LCOE) of wind and solar energy production in the US decreased by 58% and 78%, respectively [3]. Moreover, rapid deployments and considerable research and development are expected to decrease costs further—the average solar PV and onshore wind costs are predicted to reduce by a further 40–70% and 10–25%, respectively, by 2040 [2]. Electricity production is expected to meet the electric load demands of an increasingly *urbanized* world. A large proportion of the world's population already live in urban areas—in 2014, an estimated 54% of the world's population lived in urban areas, which is expected to increased further to 60% by 2030 [4]. Hence, it is important to analyze the potential for utilizing RES to meet the electricity load demand of cities. Such analyses can not only support the utilization of RES in today's cities but also the design, planning, and development of *future* 100% *RES-based "green" cities*.

In this study, we first address two general electricity-production-capacity mix questions: (1) What is the *cost-optimal electricity-production-capacity mix* to meet a city's load demand when RES—supported by battery energy storage systems (BESS)—and NRES are combined? and (2) What is the cost reduction required to enable 100% *RES-based electricity productio*n that is competitive with NRES-based electricity production? It is possible that RES-based electricity production cannot cost-effectively meet full electric loads of a city. Nevertheless, it may still cost-effectively meet *partial loads*. Therefore, we subsequently analyze and report the changes in the production costs when supplying electricity for 1–100% (discrete) time steps of the entire time period. Using our proposed methodology, planners can determine their desired RES installation and utilization based on the maximum number of hours that can be supplied by the RES and thus obtain the cost benefits of decreasing the supply security.

Further, we propose a novel methodology to analyze the impacts of exploiting the *flexible resources* present in a city. A resource is considered *flexible* if its electricity production or consumption can be shifted in time within the boundaries of end-user comfort requirements, while maintaining the total electricity production or consumption [5]. A *flexible load* thus constitutes a *shiftable por-*

tion of the total load. Cities have many potential flexible loads such as district heating facilities, electric vehicles, and potentially household devices (e.g., washing machines [6]). Hence, using a novel flexible-load methodology, we analyze the cost-effectiveness of *exploiting flexibility* by using demand-side management (DSM) to shift flexible loads as the flexible load amounts and load shift durations are varied. Our proposed flexibility model can also be generally applied to analyze the impacts of flexible loads on electricity production resources.

For our analyses, we consider RES-based "green electricity" production infrastructure comprising photovoltaic (PV) panels and wind turbines that are either centrally located outside the city borders or distributed across the city. Solar power is especially attractive as an electricity producer in cities since PV panels can be integrated into the rooftops of buildings, and potentially walls and windows as well [7]. Further, we consider Li-ion BESS, which are a well-known and highly researched solution to mitigate the variability of RES; their prices also have decreased consistently recently [8, 9]. NRES supplying "grey energy", i.e., energy from undesirable fossil fuel sources, are considered to be centralized production infrastructure located outside a city's borders. To solve these problems, we use linear programming (LP)-based innovative models that take the LCOEs of the production infrastructures, the load data of a city, and RES data—solar irradiation and wind speed—as the inputs.

Some researchers have discussed technical, economical, and political pathways to 100% cost-optimal renewable-energy production and storage for specific regions, e.g., the European Union [10], United States [11, 12], Ireland [13], Australia [14], Nigeria [15], North-East Asia [16], as well as some urban regions [17, 18, 19, 20]. Some organizations have reported transitions to sustainable energy systems in highly populated urban areas. In 2016, the National Renewable Energy Laboratory reported the potential to reach 66% renewables penetration in California, which included the roles of storage and flexibility from electric vehicles [21]. The International Renewable Energy Agency reported potential approaches toward implementing 100% sustainable urban energy systems [22]. These reports typically make qualitative analyses and focus on the technologies and methods that can be used for the transition. In contrast, our study makes a *quantitative analytical study* into the feasibility of using RES and BESS for supplying electricity to cities and presents effective techniques to analyze their viability from cost-efficiency viewpoints.

Several researchers have also focused on similar electricity generation planning problems, considering renewable energy integration [23]. Dominguez et al. [24] considered investments in both production and transmission facilities using stochastic models. Nunes et al. [25] proposed a stochastic multi-stage-planning mixed-integer linear programming (MILP) model to co-optimize generation and transmission investments under renewable targets. An MILP approach was also used by Bagheri et al. [26] to analyze the feasibility of a transition toward a 100% RES-based power system. The main difference between these studies and ours is our approach toward partial and flexible loads, especially the proposed methodology for exploiting *load flexibility* on the feasibility of large-scale RES adoption and its analyses. Although some studies considered flexible loads, their treatment was indirect, for example, by including an annual cost for load shedding [24]. Moreover, few studies have examined the possibilities of supplying < 100% renewable electrical energy (*partial* loads). Supplying partial loads is an essential component of planning electric supply not only for cities but also for small remote villages that have limited access to electricity; here, the planning problem is to offer at least some hours of electricity economically. We have made systematic investigations into how the *electric loads of cities* can be cost-optimally supplied by 100% *renewable electrical energy* by investigating *the cost impacts of* not only *full loads* but also *partial and flexible loads*.

The main contributions of our study are summarized as follows:

- We investigate the reductions in RES (wind and solar energy) and BESS costs required to make it possible for cities to be supplied by 100% RES.
- We present an LP model to determine whether RES, supported by BESS, can cost-effectively replace NRES to supply the *full loads* of cities.
- Since it may be economically feasible and attractive to meet the load demand for *a fraction* of the time period—i.e., *partial loads*—using *only green energy*, we develop a mixed-integer LP model and analyze the cost-effectiveness of meeting such partial loads.
- We solve the question of analyzing the impacts of exploiting *load flexibility* on the feasibility of large-scale RES adoption by using a *two-dimensional generalized flexibility model*. Our flexibility model is characterized by the load fraction that can be shifted to later time steps as well as the maximal *discrete* time steps across which the load fraction can be deferred. This model can also be generally applied to analyze the impacts of flexible loads on production resources.
- All our models can be universally applied to microgrid planning problems. In this study, we apply our methodology to the city of Kortrijk, Belgium, using realistic data.

Our paper is organized as follows. We first present our mathematical models and methodologies in Sec. 2. In Sec. 3, we report the results of applying our methodology to the city of Kortrijk, Belgium, as a test case. Finally, the paper is concluded in Sec. 4.

2. Mathematical Model

2.1. Renewable Energy

Wind energy was calculated from wind speeds using the Tradewind model proposed by the European Wind Energy Association [27]. An equivalent wind power curve was derived to convert wind data to energy data for wind farms across different regions in Europe.

The power production from a *solar* panel is typically given by the equation $E_{pv} = \eta \times E \times A$, where η is the energy conversion efficiency of a solar cell; E, the incident instantaneous solar irradiance (W/m^2); and A, a solar cell's surface area (m^2) [28]. We used the solar insolation I (Wh/m^2), which is the average of E over a given time period, to calculate the energy production. Standard test conditions (STC) and efficiency $\eta = 15\%$—a conventional solar panel's typical efficiency—were assumed [29]. We calculated the energy production at the given location for a solar panel per unit of surface area (m^2).

2.2. Battery Energy Storage Systems (BESS)

We considered a simplified, lossless, idealized model of battery cells whose main characteristics are the maximum energy storage capacity B_{max} (in Wh) and maximum BESS energy charge and discharge rates, k_{ch} and k_{dch} (Wh), respectively. The BESS either charges at B_{max}/k_{ch} or discharges at B_{max}/k_{dch}.

2.3. Costs

The LCOE is a common metric for comparing the cost-effectiveness of electricity generated by different sources at the point of connection to an electricity grid or load [30]. The LCOE considers the initial capital, discount rate, and the costs of continuous operation, fuel, and maintenance, and thus, they represent the full life-cycle costs of a generating plant per unit of electricity [31]. Further, the production costs of conventional power plants can be compared with those of RES. The LCOE is essentially based on a simple equation—the cost to build and operate a production asset over its lifetime divided by its total power output over that lifetime (monetary unit/kWh). Hence, we have used the LCOE as the cost parameter for our analyses. Further, we have used LCOEs from 2014 as the reference costs.

2.4. Full Loads Scenario

The problem addressed in this paper is: ***given*** *the LCOEs of green, grey, and BESS energy production, BESS characteristics, and time-series data of load, solar irradiation, and wind speed,* ***determine*** *the minimal-cost electricity production infrastructure to meet full, partial, or flexible load demands.* To solve this problem, we have used LP models with the objective of minimizing the cost of electricity production.

The objective is to minimize the cost of electricity production. For the full loads scenario, the load demand is met at all time steps. The most general case comprising all the considered production infrastructure—wind turbines, PV plants, BESS, and grey energy installations—is presented here. The decision variables are their produced energies—E_w, E_{pv}, $B_{\Delta}(t)$, and $E_g(t)$, respectively. $B_{\Delta}(t) = B_t - B_{t-1}$, where B_t is the BESS capacity (Wh) at time t. The model is as follows:

$$\min \left[\sum_{i=1}^{T} C_w \cdot f_w(W_s(t_i)) \cdot E_w + \sum_{i=1}^{T} C_{pv} \cdot f_{pv}(I(t_i)) \cdot E_{pv} + \right. \tag{1}$$

$$\left. \sum_{i=1}^{T} C_b \cdot |B_{\Delta}(t_i)| + \sum_{i=1}^{T} C_g \cdot E_g(t_i) \right] \tag{2}$$

subject to

$$f_w(W_s(t_i)) \cdot E_w + f_{pv}(I(t_i)) \cdot E_{pv} - B_\Delta(t_i) \quad + E_g(t_i) \geq E_l(t_i), \forall i = 1, ..., T \quad (3)$$

$$-B_{max}/k_{dch} \leq B_\Delta(t_i) \leq B_{max}/k_{ch}, \qquad \forall i = 1, ..., T \quad (4)$$

$$0 \leq E_w, E_{pv}, B_{max}, E_g(t_1), ..., E_g(t_T) \leq \infty \quad (5)$$

where C_w, C_{pv}, C_b, and C_g represent the LCOEs for wind, solar, BESS, and grey energy, respectively; $f_{pv}(I(t))$ and $f_w(W_s(t))$, dimensionless "black box" functions for converting irradiance $I(t)$ and wind speeds $W_s(t)$, respectively, to a fraction of the maximum possible solar and wind energy of a unit installation (1 m^2 and 1 kW installations, respectively); B_{max}, the maximum BESS capacity (kWh), T, the total time period considered; t_i, each time step; and k_{ch} and k_{dch}, the BESS charge and discharge rates, respectively.

Equation 3 ensures that the load is always met at all time steps; Eq. 4 represents the charging and discharging of the BESS; and Eq. 5 gives the lower and upper bounds of the decision variables.

The other basic scenarios—only green energy; green and grey energy; and green energy with BESS—can be easily deduced from the generalized formulation by neglecting the appropriate variables. For example, for the "green energy with BESS" scenario, the grey energy portion can be dropped from the objective function as follows:

$$\min \left[\sum_{i=1}^{T} C_w \cdot f_w(W_s(t_i)) \cdot E_w + \sum_{t=1}^{T} C_{pv} \cdot f_{pv}(I(t_i)) \cdot E_{pv} \quad + \textstyle\sum_{t=1}^{T} C_b \cdot |B_\Delta(t_i)| \right]$$

The grey energy variables can either be omitted completely, or $E_g(t_i) = 0$, $\forall i = 1, ..., T$ can be enforced.

2.5. Partial Loads Scenario

In the second scenario, only partial load demands are met, which reduces the electrical reliability of the system. We considered a well-known reliability index—the *average service availability index* (ASAI)—defined as follows [32]:

$$\text{ASAI} = \frac{(\sum N_j) \cdot T - \sum (r_j \cdot N_j)}{(\sum N_j) \cdot T}$$

where N_j is the number of customers at a location j; r_j, the annual outage time for j; and T, the total time period considered [33]. For a single location, this is equivalent to

$$\text{ASAI} = \frac{N \cdot T - r \cdot N}{N \cdot T} = \frac{T_k}{T}$$

where T_k is the total number of time steps without interruptions. ASAI $\in [0, 1]$, and in the ideal case, $ASAI = 1$.

The production now meets the load demand only during *some* discrete time steps whose total number is predefined by the ASAI. To solve this problem, the LP model is reformulated as a mixed binary LP (MBLP) model. Binary decision variables $b_i = \{b_1, ..., b_T\}$, $\forall b_i \in \mathbb{Z}_2$, are used to decide whether the load will be met ($b_i = 1$) or not ($b_i = 0$), and they determine the optimum time steps for the given ASAI. The partial loads model is therefore as follows:

$$\min \left[\sum_{i=1}^{T} C_w \cdot f_w(W_s(t_i)) \cdot E_w + \sum_{i=1}^{T} C_{pv} \cdot f_{pv}(I(t_i)) \cdot E_{pv} \right] \tag{6}$$

subject to

$$f_w(W_s(t_i)) \cdot E_w + f_{pv}(I(t_i)) \cdot E_{pv} \geq b_i \cdot E_l(t_i), \quad \forall i = 1, ..., T \tag{7}$$

$$\sum_{i=1}^{T} b_i = T_k \tag{8}$$

$$b_i \in \{0, 1\}, \quad 0 \leq E_w, E_{pv} \leq \infty \tag{9}$$

Equation 7 implies that the load is met at some selected ($b_t = 1$) time steps, and Eq. 8 ensures that the loads are always met for the given ASAI.

2.6. Flexible Loads Scenario

In this scenario, we consider the potential cost reductions that can be achieved by shifting *flexible loads* in time. We characterize flexibility by two parameters: (i) a maximal fraction δ of the load that is shifted to later time steps, and (ii) a maximal amount of time r over which the loads can be deferred. Flexible load energy $E_{fl}(t_i)$ at time t_i ($\forall i = 1, ..., T$) is then defined as $E_{fl}(t_i) = \delta E_l(t_i)$, where $\delta \in [0, 1] \subset \mathbb{R}$ and $E_l(t_i)$ is the total load. The unshiftable or inflexible load $E_{infl}(t_i) = (1 - \delta)E_l(t_i)$.

$\alpha_{i,0}$ is defined as the inflexible load fraction (unshifted load), and $\alpha_{i,1}, \alpha_{i,2}, ...\alpha_{i,r}$ are the flexible load fractions that are shifted from t_i across the subsequent r time steps t_{i+1}, t_{i+2},...,t_{i+r}, respectively; $\alpha_{i,j} \in [0, 1]$. Thus, at the i^{th} time step t_i, $E_l(t_i)$ is distributed across r time steps:

$$E_l(t_i) \quad = \quad \sum_{j=0}^{r} \alpha_{i,j} E_l(t_i) \tag{10}$$

where

$$\sum_{j=0}^{r} \alpha_{i,j} = 1$$

The load that is shifted *away* from t_i, $E_{fl}(t_i)$, is given by

$$E_{fl}(t_i) = \sum_{j=1}^{r} \alpha_{i,j} E_{fl}(t_i) \tag{11}$$

and the unshifted load energy component $E_{infl}(t_i) = \alpha_{i,0} E_l(t_i)$. A load cannot be shifted beyond the final time step, and therefore, $r + t_i \leq T$. The total flexible load that has been shifted *to* a time step t_i from previous time steps, $E^*_{fl}(t_i)$, is given by

$$E^*_{fl}(t_i) = \sum_{k=1}^{r} \alpha_{i-k,k} E_l(t_{i-k}) \tag{12}$$

Here, r prior loads from $t_{i-1}, t_{i-2}, ..., t_{i-r}$ time steps earlier have been shifted to the current time step t_i. Note that $i - k > 0$.

We will first incorporate this flexibility model into an LP formulation.

2.6.1. LP Formulation with Flexibility

We consider the "green energy with BESS" case for the production. The objective is to minimize the costs for the proposed production infrastructure mix. The LP problem is almost identical to the previous formulation (Sec. 2.4), but additional decision variables $\alpha_{i,j}$ are included. Further, the first constraint—load is met at every time step—now includes the flexible load (Eq. 12). Two additional constraints—related to $\alpha_{i,j}$—are also included.

$$min \left[\sum_{i=1}^{T} C_w \cdot f_w(W_s(t_i)) \cdot E_w + \sum_{i=1}^{T} C_{pv} \cdot f_{pv}(I(t_i)) \cdot E_{pv} \quad + \textstyle\sum_{i=1}^{T} C_b \cdot |B_\Delta(t_i)| \right]$$

subject to

$$f_w(W_s(t_i)) \cdot E_w + f_{pv}(I(t_i)) \cdot E_{pv} + B_\Delta(t_i) \geq \sum_{k=0}^{r} \alpha_{i-k,k} E_l(t_{i-k}), \quad \forall i = 1, ..., T \tag{13}$$

$$\sum_{j=0}^{r} \alpha_{i,j} = 1, \quad \forall i = 1, ..., T \tag{14}$$

$$0 \leq \alpha_{i,j} \leq 1, \;\; \forall i \in \{1, ..., T\}, \; \forall j \in \{0, ..., r\} \tag{15}$$

Equation 13 ensures that the load demand is met at all time steps, and Eqs. 14 and 15 give the bounds for $\alpha_{i,j}$. The load in Eq. 13 is the sum of $E^*_{fl}(t_i)$ (Eq. 12) and $E_{infl}(t_i)$ ($\alpha_{i,0} E_l(t_i)$). The remaining constraints pertaining to the BESS and the upper and lower bounds are identical to Eqs. 4 and 5.

The customer's load schedule should contain as few load shifts as possible, since this will cause the least inconvenience or loss of comfort. The presented LP model determines the minimal costs for a given r and δ and yields a new load schedule. However, the LP model can yield multiple solutions with equal (minimal) costs but different sets of $\alpha_{i,j}$ values. Therefore, the solution may not always be the best schedule, i.e., the schedule with the least load shifts. Hence, we implemented an additional schedule optimization step in which we use the newly derived optimum production schedule from the LP model to derive new optimum values for $\alpha_{i,j}$.

2.6.2. Flexible Schedule Optimization

We use the newly derived production schedule from the LP model to obtain new values for $\alpha_{i,j}$; the algorithm is presented in Algorithm 1. New $\alpha_{i,j}$ values—$(\alpha_n)_{i,j}$—are initially set to 0. Line 4 initializes $\alpha_{i,1}$ to δ, which implies that initially, the entire flexible load is shifted to the very next time step. In lines 5–6, the current inflexible and flexible loads are calculated. If the total production is greater than the new total load with $\alpha_{i,1} = 1$, it is not necessary to shift the loads anymore—all relevant α values are set to 0 (lines 7–8). If the total load is greater than total production, the most recent flexible loads are shifted first. If the total remaining load is still greater than the total production, the next nearest flexible loads are shifted. This process (lines 10–18) is repeated until the production at least matches the corresponding load. Lines 3–21 are then repeated for all time steps.

Note that we could have attempted to integrate the problem of deriving the best schedule into the LP model and solved a single optimization problem. However, constructing and implementing a model that not only solves the flexibility problem but also chooses the best solution is complicated and slower. Instead, from one of the many possible equal-cost solutions, i.e., the one of the many found by an LP solver, we can derive a solution with minimal shifts using our proposed algorithm (Algorithm 1).

3. Results

3.1. Experimental Data

3.1.1. Data Period

We performed our simulations for 1-year data with a data resolution of 15 minutes.

3.1.2. Location

We considered the city of Kortrijk, Belgium, which is a reasonably sized typical Belgian city with a total population of 75,219 and a population density of 940 inhabitants/km^2 (2013) [34].

3.1.3. Wind Speeds and Solar Irradiation

For the solar irradiation and wind speeds, we used 5 min measurement data obtained at Lemcko Labs, Kortrijk, Belgium [35]. Data for an entire year from September 1, 2012 to August 31, 2013 was considered, since this period covers all four seasons and enables us to investigate seasonal variations. Further, since

Algorithm 1 Flexible load schedule optimisation

Inputs: (1) the newly derived production schedule E_s; (2) the old (unshifted) load schedule E_ℓ; (3) total time period T; (4) r; and (5) δ
$i = 1$; $(\alpha_\mathrm{n})_{i,j} = 0$ $(\forall i = 1, ..., T; j = 0, ..., r)$
while $i <= T$ **do**
  $(\alpha_\mathrm{n})_{i,1} = \delta$
  $E_{infl}(t_i) = (1 - \delta)E_\ell(t_i)$
  $E_{fl}(t_i) = \sum_{j=1}^{r} (\alpha_\mathrm{n})_{i-j,j} \delta E_\ell(t_{i-j})$
  if $E_s(t_i) \geq (E_{fl}(t_i) + E_{infl}(t_i))$, **then**
    $(\alpha_\mathrm{n})_{i-1,2}, ..., (\alpha_\mathrm{n})_{i-r,r} = 0$
  else
    while $E_s(t_i) < (E_{fl}(t_i) + E_{infl}(t_i))$, **do**
      for j = i-1:-1:i-r+1 **do**
        $E_x(t_i) = (E_{fl}(t_i) + E_{infl}(t_i)) - E_s(t_i)$
        $(\alpha_\mathrm{n})_{j,i-j+1} =$
        $min\{E_x(t_i)/\delta E_\ell(t_j), (\alpha_\mathrm{n})_{j,i-j}\}$
        $(\alpha_\mathrm{n})_{(j,i-j)} = (\alpha_\mathrm{n})_{(j,i-j)} - (\alpha_\mathrm{n})_{(j,i-j+1)}$
        $E_x(t_i) = E_x(t_i) - (\alpha_\mathrm{n})_{(j,i-j+1)} \delta E_\ell(t_j)$
      end for
    end while
  end if
  $i = i + 1$
end while
Output: $(\alpha_\mathrm{n})_{i,j}$ $(\forall i = 1, ..., T; j = 0, ..., r - 1)$

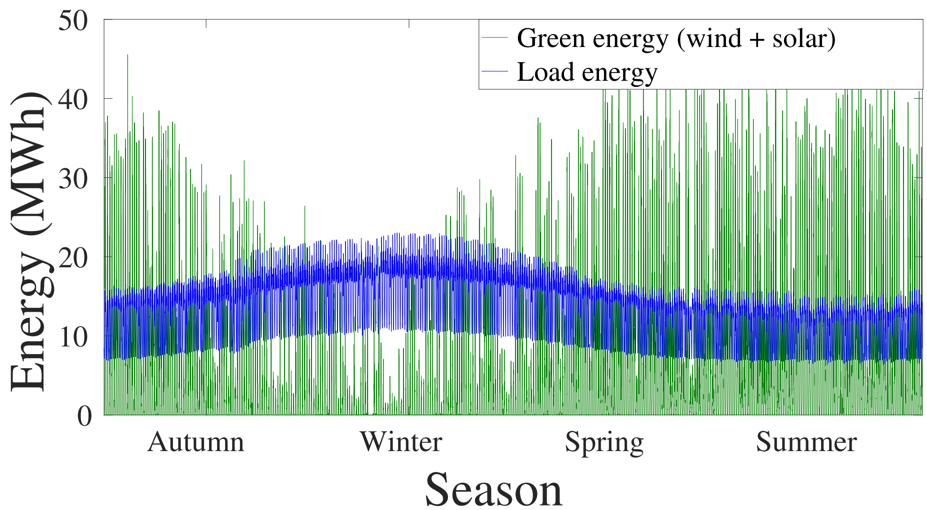

Figure 1: Input load energy data and renewable ("green") energy production data (assuming 1 MW solar and wind power plants) for a year at Kortrijk, Belgium (15 min time resolution).

load data was available only at 15 min intervals, we aggregated the 5 min data for wind speeds and solar irradiation into 15 min data.

3.1.4. BESS

We considered lithium-ion (Li-ion) batteries because they are among the most promising next-generation batteries for supporting renewable energy-based production [36]. Li-ion cells offer the best cycle efficiency (90%) and durability, lowest self-discharge (5–8% per month at 21°C), and energy density (up to 630 Wh/l) [36]. Further, Li-ion batteries are expected to become cheaper in the future [9]. We considered charge and discharge rates of 1C, which implies that the BESS charges and discharges at its maximum capacity at every time step.

3.1.5. Load

In Belgium, the meter readings of most customers are not recorded continuously, and synthetic load curves (SLPs) are used to estimate the energy consumption. We used the SLP provided by the Flemish Regulation Entity for the Electricity and Gas market (VREG) for 2012–13 [37]. These SLP profiles model typical user consumption using statistical averages on real life data, as measured by the VREG, and give the amount of energy consumed at 15 min intervals. Figure 1 shows the input load data and the renewable energy production data (assuming solar and wind power plants with nominal power plant capacity of 1 MW) used in this study for a year.

3.1.6. Costs

For LCOE data, we considered a pan-European study conducted by the European Commission that reported energy cost data of different electricity and heat technologies for all countries in the European Union [38]. The LCOEs of small rooftop PV systems, which are popular in Belgium, and onshore wind power were 0.130 €/kWh and 0.110 €/kWh, respectively. The Belgian electricity production infrastructure comprises nuclear (39.54%), natural gas (33.96%), coal (3.14%), liquid fuel (1.5%), water (9.3%), wind (5.93%), and others (6.64%). We calculated the grey energy LCOE as a proportion of their contributions to the total energy as 0.0386 €/kWh. The procedures for calculating the LCOEs are given in detail in Annexure 4 of the report published in [38].

Unfortunately, the European Commission study did not include BESS costs. Consequently, we examined scenarios in other countries and concluded that the Li-ion BESS LCOE is currently about 5 times that of wind [3]. Hence, we applied a factor of 5 to the European wind LCOE and arrived at a BESS LCOE of 0.55 €/kWh.

3.2. Results

3.2.1. Basic Scenarios

The "only green" scenario was expectedly infeasible throughout the year. Further, green energy and BESS have no impacts when grey energy is included since they are much more expensive.

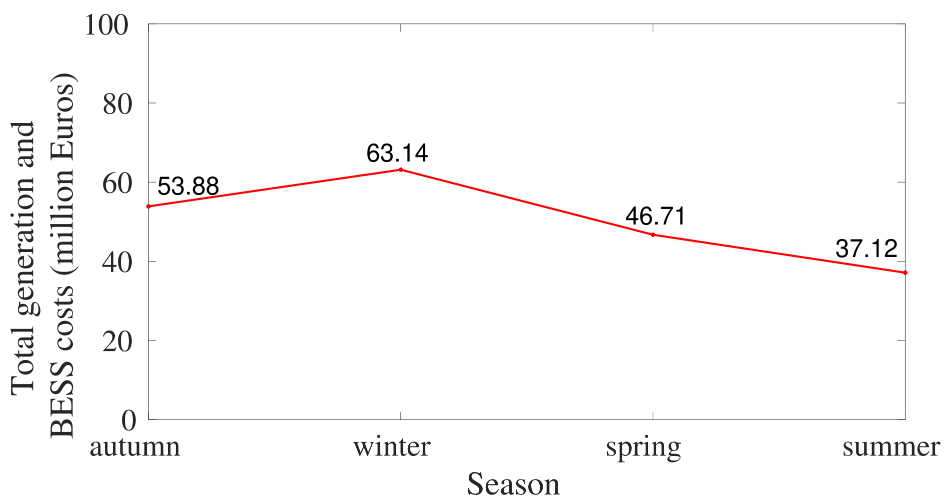

Figure 2: Seasonal variations in the total actual costs for the "green–battery energy storage system (BESS)" case; the costs when grey energy was included were about 4.6, 5.49, 4.54, and 3.85 million Euro for the four seasons, respectively.

Figure 2 shows the seasonal variations in the total costs for the "green–BESS" case. The average cost per unit of electricity produced was 0.4520, 0.4442,

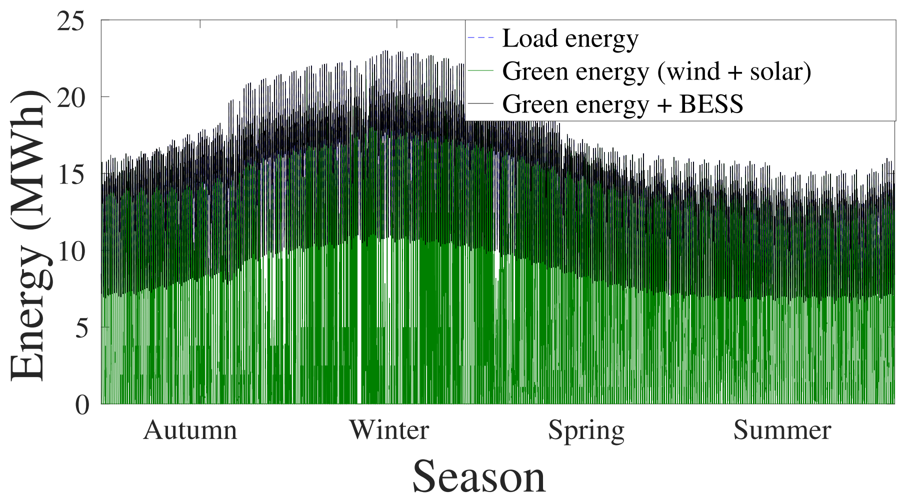

Figure 3: Green–BESS energy production meeting the load nearly perfectly. The curtailment is negligible and the dotted line representing the load (compare with Fig. 1 showing input data) is almost completely covered by the combined supply from green energy and BESS, shown in black.

0.3972, and 0.3720, €/kWh for autumn, winter, spring, and summer, respectively. The costs were lowest in summer due to lower load demand and more renewable resources and highest in the winter. When grey energy was included, it was dominantly selected due to its low costs, and the production infrastructure became cheaper by a factor of ≈ 12—the yearly cost with BESS, for example, was 204.15 million Euro (average cost of 0.4265 €/kWh), while it was 18.47 million Euro with grey energy (average cost of 0.0386 €/kWh, i.e., its LCOE). Note that this can also be predicted from their LCOEs (grey energy is about 14 times cheaper than BESS). When BESS is used with green energy, any excess produced green energy is stored in the BESS to be used at later times with insufficient green energy production (Fig. 3). The curtailment is negligible and the load (dotted blue lines; compare with Fig. 1 showing input data) is almost completely covered by the combined supply from green energy and BESS (black lines). The sizing algorithm is designed to dimension a sufficiently large BESS capacity that ensures that the produced electricity is not wasted due to RES curtailment.

Figure 4 shows the green energy production, which is *directly used without storing* in the BESS, and cost as a proportion of the total. Green energy proportion was highest in summer (nearly 30%) and lowest in winter and autumn, halving to nearly 15%.

3.2.2. Cost Variations

In the LP solution, grey energy is dominantly selected over the other alternatives due to its significantly lower cost. However, continuous innovations and research and development are making RES increasingly cost-competitive with

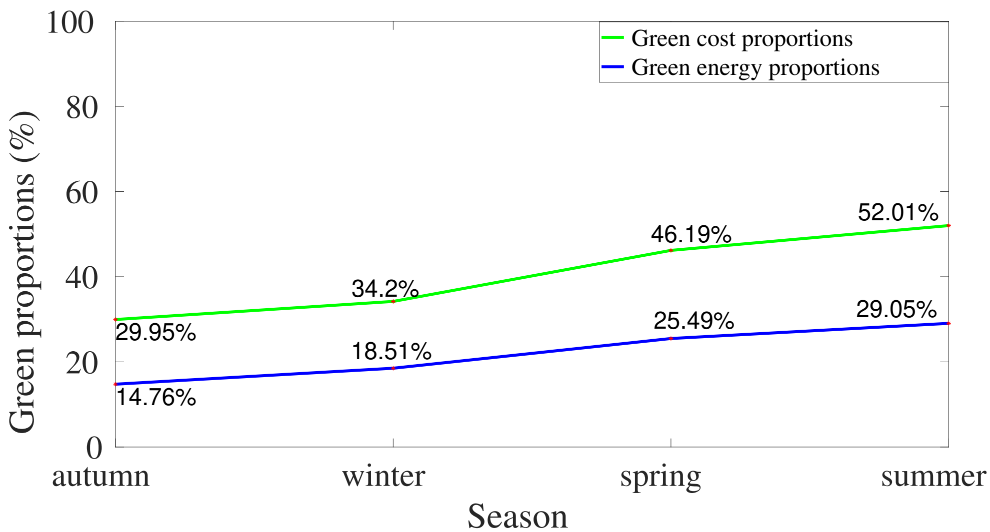

Figure 4: Green energy production and cost proportions (%)—directly used without storing in BESS—for the "green–BESS" case.

fossil fuels. Hence, we investigated the increase in green energy proportions, i.e., its participation, as the costs of RES and BESS decrease, when grey energy is included.

Figure 5 shows the variations in green energy as a proportion of the total energy when green and BESS LCOEs are varied from 0–40% and 0–25% of their reference costs, respectively. The green energy includes the energy shifted by the BESS. Green energy participation is negligible when the green energy costs are $\geq$ 40% of the reference costs, i.e., $\geq$0.044 €/kWh. Without the BESS, the maximum green energy proportion is 63%, which is the maximum ASAI (or the maximum amount of load) that can be met by RES alone. With the BESS, the green energy proportion is 100% when the BESS cost is $\leq$ 7% of the reference costs, i.e., $\leq$ 0.038 €/kWh. Thus, the BESS costs must significantly decrease to enable affordable 100% RES.

At the same time, grey energy costs could also increase, for example, if EU emissions trading system (EU ETS) is considered. Figure 6 shows the variations in green, grey, and BESS energy as a proportion of the total energy required to meet the load when grey energy costs are varied from 1–20 times their reference costs. Green energy participation is negligible until around 3$\times$ the grey energy reference costs, i.e., $\approx$ 0.1158 €/kWh after which its proportion of the total energy increases. When grey energy costs are 15$\times$ the reference costs, i.e., $\geq$0.5790 €/kWh, it becomes economical to use BESS to support the green energy production. As a result, grey energy is not required any more and it is possible to supply electricity with 100% green energy supported by BESS.

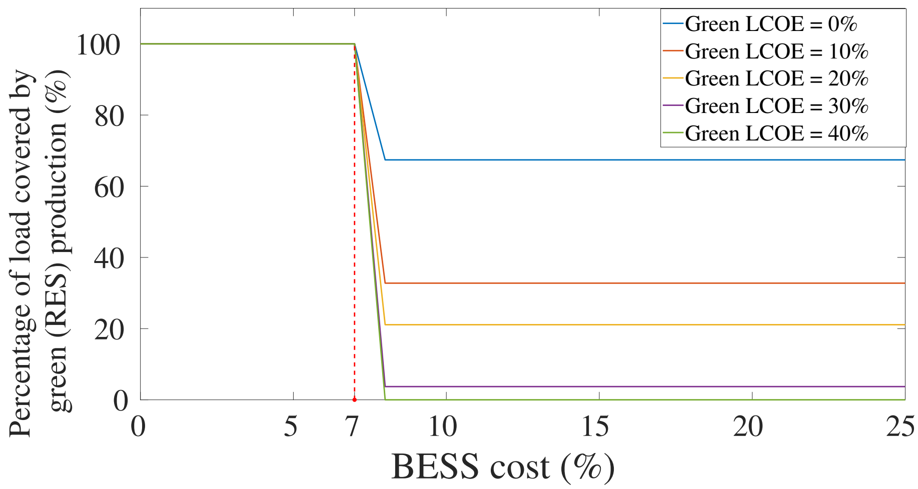

Figure 5: Variations in the proportion of green energy production in the "green–BESS–grey" scenario, when BESS energy costs were changed from 0–100% of its current costs.

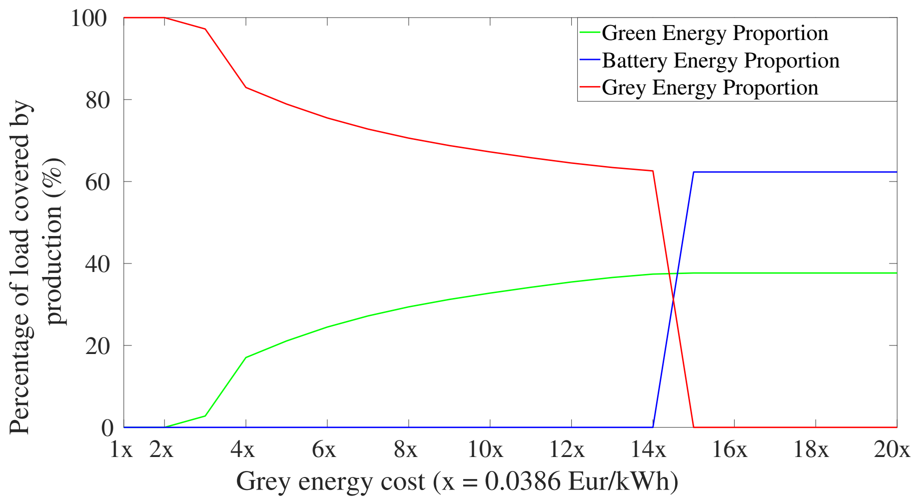

Figure 6: Variations in the proportion of green, grey, and BESS energy production in the "green–BESS–grey" scenario, when green energy costs were changed from 1–20 times of its current reference costs.

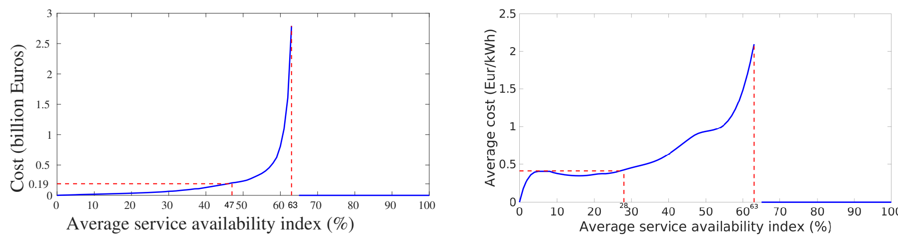

(a) ASAI versus total cost (b) ASAI versus average cost

Figure 7: Average service availability index (ASAI) versus cost for green energy alone, for the entire year; the maximum ASAI is 63% above which green energy alone cannot meet the load demand. For ASAI $\leq$ 47%, the *total cost* of using green energy alone ($\leq$ 190 million Euro) is less than the cost of using green energy with BESS (204 million Euro); the minimal-cost installation will not use BESS. Similarly, for ASAI $\leq$ 28%, the *average cost* of using green energy alone (0.4238 €/kWh) is lesser than the cost of using green energy with BESS (0.4265 €/kWh).

3.2.3. Partial Loads—ASAI

The maximum ASAIs using only RES were 50%, 57%, 73%, and 73% for autumn, winter, spring, and summer, respectively. Unsurprisingly, the summer season had the best electrical reliability (in terms of ASAI) and lowest costs. The maximum ASAI for the entire year was 63%, which implies that it was possible to meet the entire load for only 63% of the given time period. Figure 7a shows the changes in the total production cost with the ASAI. The total cost increases nearly exponentially above the ASAI of $\approx$ 40% until the maximum ASAI of 63% because of the extreme installation sizes (and thus, costs) required to meet the load at times steps with low wind speeds and solar irradiation. When ASAI $\leq$ 50%, the total cost is one-tenth of the cost required to meet the maximum ASAI. For ASAI $\leq$ 47%, the total cost of using green energy alone ($\leq$ 190 million Euro) is less than the total cost of using green energy with BESS (204 million Euro). The average cost also exhibits similar trends (Fig. 7b); for an ASAI of 1–30%, the average cost is $<$ 0.4538 €/kWh, increasing to 2.0981 €/kWh at 63%. When ASAI $\leq$ 50%, the average cost is less than half the average cost required to meet the maximum ASAI. Moreover, for ASAI $\leq$ 28%, the average cost of using green energy alone (0.4238 €/kWh) is less than the average cost of using green energy with BESS (0.4265 €/kWh). On the other hand, the average cost even at ASAI = 1% is more than that using grey energy alone. These results suggest that even at the reference costs and with limited installed capacity, it is possible for planners desiring to use *only* green energy to dramatically decrease the costs if they tolerate meeting the load demand for at least 50% of the time, while using other energy resources for the remaining time.

Figure 8a shows the curtailed energy versus ASAI. As shown, a significant proportion of the produced energy is curtailed in this scenario. This is because

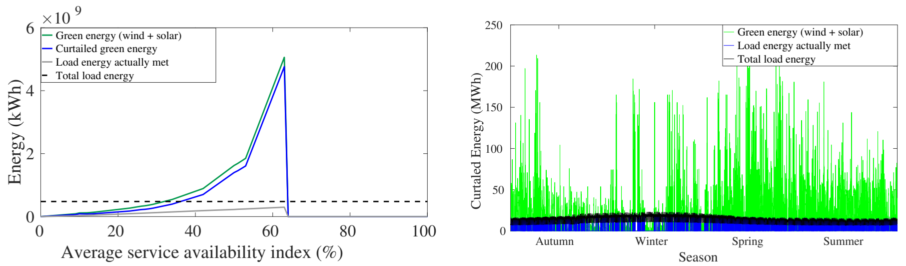

(a) Curtailed energy versus ASAI.

(b) Example of the curtailment of produced energy (ASAI = 25%).

Figure 8: Curtailed energy in the only "green energy" scenario.

if the load has to be met for a high proportion of the total time period, the green energy infrastructure must be dimensioned very large to still produce sufficient power at times when the available green resources (i.e., wind speed and solar irradiation) are very low. Hence, the infrastructure is over-dimensioned and produces excessive energy when the available green resources are plentiful. Figure 8b illustrates an example of the curtailment of produced energy for ASAI of 25%. At some time steps, the green energy just meets the load energy whereas there is excessive production at other time steps.

3.2.4. Flexible Loads

Figure 9 shows the minimal costs for the "green–BESS" scenario with flexible loads. $r = 48$ implies that the loads can be shifted over maximally 48×15 min $=$ 12 h. For all flexible load proportions δ, the cost was 204 million Euros when there was no shift ($r = 0$), which agrees with the yearly costs for basic dimensioning. Naturally, the costs were lowest when the entire load can be shifted, i.e., $\delta = 100\%$. As the maximal amount of time shifting, r, increases, the costs decrease, but this decrease slows down with higher r, which suggests that shifting the load is beneficial only up to a certain time frame. However, the costs do not decrease sufficiently to reach the low costs offered by grey energy installations (about 18.47 million Euro). This suggests that today, load shifting is not competitive with grey energy production to counterbalance intermittent renewable energy production.

Figure 10 illustrates the applied (minimal) time shifts for $\delta = 40\%$ and $r = 12$ (3 h). At least 60% ($= 1 - \delta$) of the load is unshifted, whereas maximally 40% of the load can be shifted. A histogram of the fractions of the total load shifted (%) for each of the possible time shifts up to 12 for a year is presented. The scheduling algorithm shifted nearly 35% of the total load to the first time step (15 min), and very few loads were shifted beyond 4 time steps (1 h). This suggests that large time shifts are rarely useful (for balancing).

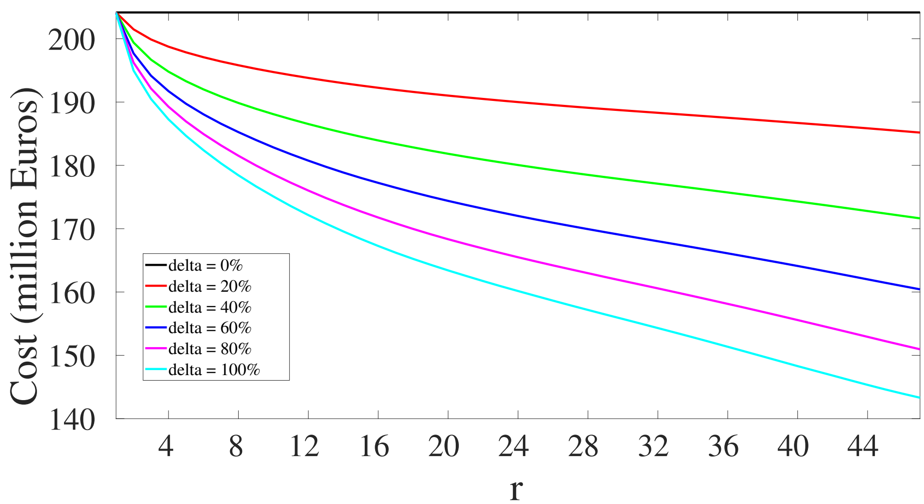

Figure 9: Variations in the minimal cost in the "green–BESS" scenario when the load is shifted with r varied from 1–12 h and δ from 0–100%; the cost when grey energy was included was 18.47 million Euro. r refers to the maximal number of 15-min time steps over which the total load can be distributed.

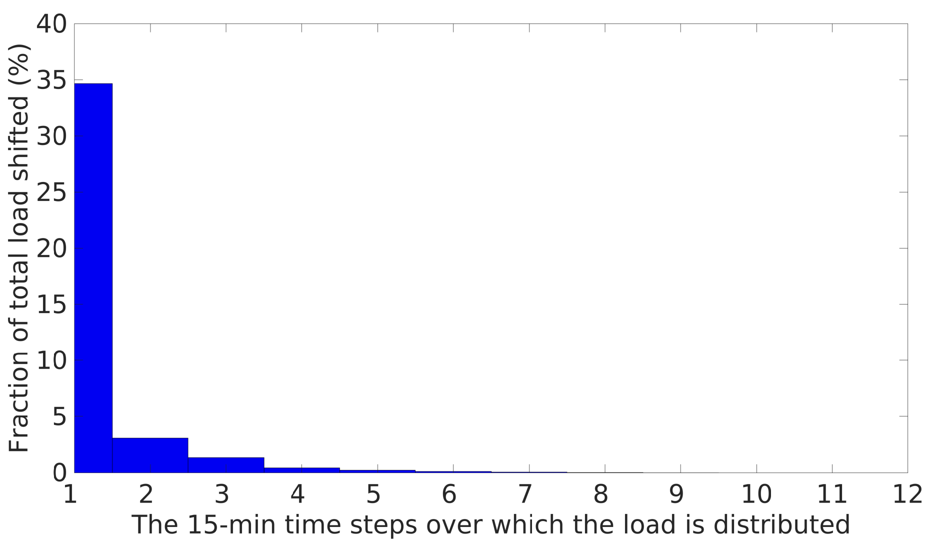

Figure 10: Histogram of the fractions of the total load (%) shifted across 1–r time steps for a year. Here, $\delta = 40\%$ and $r = 12$ were chosen to illustrate the performance of Algorithm 1. About 60% of the total load is unshifted and nearly 35% is now shifted to the first time step (15 min); very few loads are shifted beyond 4 time steps (1 h).

4. Conclusions

In this paper, we investigated the cost-effectiveness of meeting the load demands of cities with 100% RES from PV panels and wind turbines, supported by BESS. We developed an LP-based methodology and applied it to the loads of Kortrijk, a Belgian city with around $75,000$ inhabitants.

We first obtained the cost-optimal electricity-production-infrastructure mix to meet a city's full load demand when RES—supported by BESS—and NRES are combined. Since the LCOEs of RES and BESS were higher than the LCOE of NRES, they were *not selected* in the minimal-cost solution for supplying electrical energy to a city. Moreover, with the reference costs, the RES–BESS system costs were about $10\times$ times *higher* than when NRES was included. The costs were expectedly lowest in summer and highest in winter. Green energy production alone—without BESS—was able to meet 63% of the load demand, but for RES systems to become competitive with NRES, their costs must decrease. Note that green energy alone could meet only 63% of the load because the available green resources (i.e., wind speeds and solar irradiation) were 0 for 37% of the total time period. These results will not only differ for different cities but also be influenced by technological developments. For example, the adoption of low-speed wind turbine technology will increase the available hours for wind power.

We then analyzed the question of how much the cost must decrease to enable 100% *RES-based electricity productio*n to be competitive with NRES-based electricity production. At 40% of the reference costs used in the paper, i.e., at ≈ 0.044 €/kWh, RES would meet 63% of the load demand more profitably than NRES. Further, the production cost with RES alone reduces nearly exponentially with lower ASAI and, for ASAI $\leq 50\%$, it is one-tenth of the cost with maximum ASAI (63%). Thus, even at the reference cost, it is possible to cost-effectively meet nearly 50% of the load demand using RES alone at 10% of the production costs required to meet 63% of the load demand. Moreover, the total and average costs of using RES alone were less than the cost of using RES with BESS at ASAI of 47% and 28%, respectively. For BESS to be cost effective, its cost needs to reduce to around 7% of the reference costs, i.e., ≈ 0.038 €/kWh. An RES-BESS system with these costs—≈ 0.044 €/kWh and ≈ 0.038 €/kWh, respectively—will meet 100% of the load demand more cost-effectively than NRES. We also analyzed the effects of increasing the costs of NRES on the adoption of green energy. Green energy participation begins to increase as the grey energy costs become $\geq 3\times$ the grey energy reference costs (≈ 0.1158 €/kWh). And, at a $15\times$ increase of the reference costs ($\geq$0.5790 €/kWh), grey energy is not required anymore and it is more economical to adopt green energy with BESS.

Finally, we analyzed how exploitation of *the flexible resources* present in a city improves the cost-effectiveness of RES deployment by investigating the effects of electrical load shifting. We developed and employed a novel two-step flexible-load analysis to explore the changes in the minimal costs with the amount of shifted load fractions (δ) and the maximal *discrete* time steps

(r) across which the load fractions can be shifted. As r increased, the costs *decreased* by nearly 20% until around 3–5 h, after which it remained nearly constant. Nevertheless, the costs for RES–BESS system with load shifting—around 170 million Euro—were higher than the costs for only NRES system—18.47 million Euro, implying that load shifting with RES–BESS system alone is not competitive with grey costs today. Our results show that it is most economical to not use RES today even when the loads are flexible. However, when the costs of RES and BESS reach around 0.044 and 0.038 €/kWh, respectively, it will become possible to cost-effectively supply the entire load of a city using RES (with BESS).

These results suggest that it is very important to integrate several renewable energy sectors—electricity, heat, transport, etc.—to reach high levels of RES penetration, and they agree with the growing consensus that *smart energy systems* offer better options for integration of renewable energy into energy systems [39, 40]. Moreover, the flexibility that can be exploited in the electricity system alone is clearly limited without integrating co-generation and transportation [41]. Nevertheless, the presented methodologies are valuable because they can be simply and effectively used to investigate the utilization and meaningful rate of adoption of RES technologies. The partial-loads analysis shows that the costs required to meet the load demand decrease dramatically with decreasing ASAI. This represents a significant opportunity to meet at least a portion of a city's load at relatively low costs using RES alone. Further, the methodology itself is useful to decide how many hours can be met with RES, given a certain budget. It can also be used in rural areas for providing at least partial access to electricity. Our flexibility model can be generally applied to analyze the impacts of flexible loads on production resources, and it can also be a valuable tool for analyzing the economic value of DSM algorithms. These models can be easily expanded to include flexibilities arising from the integration of other sectors as well.

In the future, we plan to model cost evolutions over a long time period; further, we will incorporate communication costs and other externalities in our algorithm for exploiting flexibility.

Acknowledgment

We are grateful to the Lemcko research group (Ghent University) for kindly providing us with large data sets for the Belgium test case. We gratefully acknowledge the generous computational resources (Stevin Supercomputer Infrastructure) and services provided by the VSC (Flemish Supercomputer Center), funded by the Research Foundation - Flanders (FWO) and the Flemish Government—department EWI, as well as by the CSC–IT Center for Science, Finland.

References

[1] European Council, 2030 Climate and Energy Policy Framework, Tech. rep., European Commission, Brussels (Oct. 2014).

URL http://www.consilium.europa.eu/uedocs/cms_data/docs/pressdata/en/ec/145397.pdf

[2] International Energy Agency, World Energy Outlook 2016—Executive Summary, Tech. rep., International Energy Agency, Paris (Nov. 2016). URL http://www.iea.org/newsroom/news/2016/november/world-energy-outlook-2016.html

[3] Lazard, Levelized Cost of Energy Analysis Version 8, Tech. rep. (Sep. 2014). URL www.lazard.com

[4] United Nations, World Urbanization Prospects (Highlights), Tech. rep., New York (2014). URL http://esa.un.org/unpd/wup/Highlights/

[5] Pamela MacDougall, Bart Roossien, Cor Warmer, Koen Kok, Quantifying flexibility for smart grid services, in: Power and Energy Society General Meeting (PES), 2013 IEEE, Vancouver, Canada, 2013, pp. 1–5. doi:10.1109/PESMG.2013.6672817.

[6] N. Sadeghianpourhamami, T. Demeester, D. Benoit, M. Strobbe, C. Develder, Modeling and analysis of residential flexibility: Timing of white good usage, Appl. Energy 179 (2016) 790–805. doi:10.1016/j.apenergy.2016.07.012. URL http://linkinghub.elsevier.com/retrieve/pii/S0306261916309539

[7] E. Cuce, Toward multi-functional PV glazing technologies in low/zero carbon buildings: Heat insulation solar glass—Latest developments and future prospects, Renew. Sustain. Energy Rev. 60 (2016) 1286–1301. doi:10.1016/j.rser.2016.03.009. URL http://linkinghub.elsevier.com/retrieve/pii/S1364032116002446

[8] M. Beaudin, H. Zareipour, A. Schellenberglabe, W. Rosehart, Energy storage for mitigating the variability of renewable electricity sources: An updated review, Energy for Sustain. Dev. 14 (4) (2010) 302–314. doi:10.1016/j.esd.2010.09.007.

[9] International Renewable Energy Agency, Battery Storage for Renewables: Market Status and Technology Outlook, Tech. rep., International Renewable Energy Agency, Abu Dhabi (Jan. 2015).

[10] D. Connolly, H. Lund, B. Mathiesen, Smart Energy Europe: The technical and economic impact of one potential 100% renewable energy scenario for the European Union, Renew. and Sustain. Energy Rev. 60 (2016) 1634–1653. doi:10.1016/j.rser.2016.02.025. URL http://linkinghub.elsevier.com/retrieve/pii/S1364032116002331

[11] T. Mai, D. Mulcahy, M. M. Hand, S. F. Baldwin, Envisioning a renewable electricity future for the United States, Energy 65 (2014) 374–386. doi:10.1016/j.energy.2013.11.029.
URL http://linkinghub.elsevier.com/retrieve/pii/S0360544213009912

[12] T. Mai, M. M. Hand, S. F. Baldwin, R. H. Wiser, G. L. Brinkman, P. Denholm, D. J. Arent, G. Porro, D. Sandor, D. J. Hostick, M. Milligan, E. A. DeMeo, M. Bazilian, Renewable electricity futures for the United States, IEEE Trans. on Sustain. Energy 5 (2) (2014) 372–378. doi:10.1109/TSTE.2013.2290472.
URL http://ieeexplore.ieee.org/document/6690152/

[13] D. Connolly, B. V. Mathiesen, A technical and economic analysis of one potential pathway to a 100% renewable energy system, International J. of Sustain. Energy Plan. and Management 1 (2014) 7–28.
URL http://journals.aau.dk/index.php/sepm/article/view/497

[14] A. Blakers, B. Lu, M. Stocks, 100% renewable electricity in Australia, Energy 133 (2017) 471–482. doi:10.1016/j.energy.2017.05.168.
URL http://linkinghub.elsevier.com/retrieve/pii/S0360544217309568

[15] U. B. Akuru, I. E. Onukwube, O. I. Okoro, E. S. Obe, Towards 100% renewable energy in Nigeria, Renew. and Sustain. Energy Rev. 71 (2017) 943–953. doi:10.1016/j.rser.2016.12.123.
URL http://linkinghub.elsevier.com/retrieve/pii/S1364032116311716

[16] D. Bogdanov, C. Breyer, North-East Asian Super Grid for 100% renewable energy supply: Optimal mix of energy technologies for electricity, gas and heat supply options, Energy Convers. and Management 112 (2016) 176–190. doi:10.1016/j.enconman.2016.01.019.
URL http://linkinghub.elsevier.com/retrieve/pii/S0196890416000364

[17] T. Ma, P. A. Østergaard, H. Lund, H. Yang, L. Lu, An energy system model for Hong Kong in 2020, Energy 68 (2014) 301–310. doi:10.1016/j.energy.2014.02.096.
URL http://linkinghub.elsevier.com/retrieve/pii/S0360544214002436

[18] D. Dominković, I. Bačeković, D. Sveinbjörnsson, A. Pedersen, G. Krajačić, On the way towards smart energy supply in cities: The impact of interconnecting geographically distributed district heating grids on the energy system, Energy 137 (2017) 941–960. doi:10.1016/j.energy.2017.02.162.
URL http://linkinghub.elsevier.com/retrieve/pii/S0360544217303456

[19] L. Liu, T. Zhu, Y. Pan, H. Wang, Multiple energy complementation based on distributed energy systems—Case study of Chongming county, China, Appl. Energy 192 (2017) 329–336. doi:10.1016/j.apenergy.2016.07.049.
URL http://linkinghub.elsevier.com/retrieve/pii/S0306261916309904

[20] H. Ali, S. Sanjaya, B. Suryadi, S. Weller, Analysing CO_2 emissions from Singapore's electricity generation sector: Strategies for 2020 and beyond, Energy 124 (2017) 553–564. doi:10.1016/j.energy.2017.01.112.
URL http://linkinghub.elsevier.com/retrieve/pii/S0360544217301196

[21] P. Denholm, R. Margolis, Energy storage requirements for achieving 50% solar photovoltaic energy penetration in California, Tech. rep., NREL (National Renewable Energy Laboratory (NREL), Golden, Colorado (United States) (2016).
URL https://www.nrel.gov/docs/fy16osti/66595.pdf

[22] J. Rigter, D. Saygin, G. Kieffer, Renewable Energy in cities (Oct. 2016).
URL http://www.irena.org/DocumentDownloads/Publications/IRENA_Renewable_Energy_in_Cities_2016.pdf

[23] R. Hemmati, R.-A. Hooshmand, A. Khodabakhshian, Comprehensive review of generation and transmission expansion planning, IET Generation, Transmission & Distribution 7 (9) (2013) 955–964. doi:10.1049/iet-gtd.2013.0031.
URL http://digital-library.theiet.org/content/journals/10.1049/iet-gtd.2013.0031

[24] R. Dominguez, A. J. Conejo, M. Carrion, Toward fully renewable electric energy systems, IEEE Trans. on Power Syst. 30 (1) (2015) 316–326. doi:10.1109/TPWRS.2014.2322909.
URL http://ieeexplore.ieee.org/document/6820787/

[25] J. B. Nunes, N. Mahmoudi, T. K. Saha, D. Chattopadhyay, A multi-stage transition toward high renewable energy penetration in Queensland, Australia, IET Generation, Transmission & Distribution 12 (4) (2018) 850–858. doi:10.1049/iet-gtd.2017.0930.
URL http://digital-library.theiet.org/content/journals/10.1049/iet-gtd.2017.0930

[26] A. Bagheri, V. Vahidinasab, K. Mehran, A novel multiobjective generation and transmission investment framework for implementing 100% renewable energy sources, IET Generation, Transmission & Distribution 12 (2) (2018) 455–465. doi:10.1049/iet-gtd.2017.0976.
URL http://digital-library.theiet.org/content/journals/10.1049/iet-gtd.2017.0976

[27] J. R. McLean, G. Hassan, Tradewind project, WP 2.6 Equivalent wind power curves, TradeWind Deliverable 2 (2008) 1–14. URL http://trade-wind.eu/fileadmin/documents/publications/D2.4_Equivalent_Wind_Power_Curves_11914bt02c.pdf

[28] J. V. Paatero, P. D. Lund, Effects of large-scale photovoltaic power integration on electricity distribution networks, Renew. Energy 32 (2) (2007) 216–234. doi:10.1016/j.renene.2006.01.005.

[29] International Energy Agency, Technology Roadmap, Solar Photovoltaic Energy, Tech. rep., International Energy Agency, Paris (2014).

[30] K. Branker, M. Pathak, J. Pearce, A review of solar photovoltaic levelized cost of electricity, Renew. and Sustain. Energy Rev. 15 (9) (2011) 4470–4482. doi:10.1016/j.rser.2011.07.104.

[31] F. Ueckerdt, L. Hirth, G. Luderer, O. Edenhofer, System LCOE: What are the costs of variable renewables?, Energy 63 (2013) 61–75. doi:10.1016/j.energy.2013.10.072.

[32] A. Chowdhury, S. Agarwal, D. Koval, Reliability modeling of distributed generation in conventional distribution systems planning and analysis, IEEE Trans. on Industry Appl. 39 (5) (2003) 1493–1498. doi:10.1109/TIA.2003.816554.

[33] R. Billinton, W. Li, Basic Concepts of Power System Reliability Evaluation, in: Reliability Assessment of Electrical Power Systems Using Monte Carlo Methods, 1st Edition, Plenum Press, New York, 1994, pp. 28–29.

[34] Belgian Federal Government, Population density, Belgium (April 07 2015). URL http://statbel.fgov.be/nl/modules/publications/statistiques/bevolking/bevolking_cijfers_bevolking_2010-2012.jsp

[35] Lemcko, Lemcko Energy and Power Quality (April 07 2015). URL http://www.lemcko.be/

[36] B. Diouf, R. Pode, Potential of lithium-ion batteries in renewable energy, Renew. Energy 76 (2015) 375–380. doi:10.1016/j.renene.2014.11.058. URL http://linkinghub.elsevier.com/retrieve/pii/S0960148114007885

[37] VREG, Flemish regulation entity for the electricity and gas market (2015). URL http://www.vreg.be/nl/uw-gids-op-de-energiemarkt

[38] S. Alberici, S. Boeve, P. van Breevoort, Y. Deng, S. Förster, A. Gardiner, V. van Gastel, K. Grave, H. Groenenberg, D. de Jager, E. Klaassen, W. Pouwels, M. Smith, E. de Visser, T. Winkel, K. Wouters, Subsidies and costs of EU energy, Tech. rep., European C ommission, Directorate - General for Energy (Nov. 2014).

URL https://ec.europa.eu/energy/en/content/final-report-ecofys

[39] H. Lund, A. N. Andersen, P. A. Østergaard, B. V. Mathiesen, D. Connolly, From electricity smart grids to smart energy systems—A market operation based approach and understanding, Energy 42 (1) (2012) 96–102. doi:10.1016/j.energy.2012.04.003.
URL http://linkinghub.elsevier.com/retrieve/pii/S0360544212002836

[40] H. Lund, P. A. Østergaard, D. Connolly, I. Ridjan, B. V. Mathiesen, F. Hvelplund, J. Z. Thellufsen, P. Sorknæs, Energy storage and smart energy systems, International J. of Sustain. Energy Plan. and Management 11 (2016) 3–14.

[41] P. S. Kwon, P. Østergaard, Assessment and evaluation of flexible demand in a Danish future energy scenario, Appl. Energy 134 (2014) 309–320. doi:10.1016/j.apenergy.2014.08.044.
URL http://linkinghub.elsevier.com/retrieve/pii/S0306261914008472